

## Vibrational fine structure in the Si $2p$ photoelectron spectra of simple gaseous molecules

J. D. Bozek, G. M. Bancroft, and K. H. Tan

*Department of Chemistry and Center for Chemical Physics, University of Western Ontario, London, Ontario, Canada N6A 5B7  
and Canadian Synchrotron Radiation Facility, Synchrotron Radiation Center, University of Wisconsin,  
Stoughton, Wisconsin 53589*

(Received 16 November 1990)

The silicon  $2p$  photoelectron spectra of eleven molecules:  $\text{SiH}_4$ ,  $\text{Si}(\text{CH}_3)_4$ ,  $\text{C}_2\text{H}_5\text{SiH}_3$ ,  $(\text{CH}_3)_2\text{SiH}_2$ ,  $(\text{CH}_3)_3\text{SiH}$ ,  $\text{SiF}_4$ ,  $\text{SiCl}_4$ ,  $(\text{CH}_3)_3\text{SiCl}$ ,  $(\text{CH}_3)_3\text{SiI}$ ,  $\text{Cl}_2\text{SiH}_2$ , and  $\text{CH}_3\text{SiF}_3$ , have been recorded at high experimental resolution. The spectra all exhibit broadening, and in some cases resolved fine structure resulting from the excitation of vibrations in the core-ionized molecules. Extensive use is made of the equivalent-cores approximation to aid in the interpretation of the observed vibrational structure. Chemical effects on the lifetime of the Si  $2p$  core holes are postulated for the alkyl-silane molecular series and  $\text{SiF}_4$  based on the linewidths obtained from deconvolutions of the experimental spectra with manifolds of vibrational bands.

### I. INTRODUCTION

Vibrational fine structure in molecular core-level spectroscopy was first resolved in the  $\text{C}1s$  photoelectron spectrum of  $\text{CH}_4$  reported by Siegbahn.<sup>1</sup> The spectrum was measured with a monochromatized Al  $K\alpha$  source yielding a total experimental resolution of  $\sim 0.4$  eV and it was observed to be noticeably asymmetric exhibiting three unresolved vibrational bands of decreasing intensity.<sup>1</sup> The resolution of the spectrometer was subsequently slightly improved and the vibrational progression was resolved into its individual bands.<sup>2</sup> Prior to Siegbahn's measurements, core-level photoelectron bands were not expected to exhibit vibrational fine structure<sup>3,4</sup> since core orbitals are generally considered nonbonding orbitals and, based on trends observed in the vibrational structure accompanying valence photoelectron bands, photoelectron bands of nonbonding orbitals do not exhibit vibrational fine structure.<sup>5</sup>

Numerous other examples of vibrational fine structure have since been observed in core-level spectra using a variety of different experimental techniques. Absorption techniques (photoabsorption, electron energy loss, and photoelectron spectroscopies) and emission techniques (x-ray emission, Auger, and autoionization spectroscopies) have both been used to study the vibrational bands observed in core-level spectroscopy. In absorption-type experiments, the core-ionized molecule is the final state of the experiment. The attenuation of the incident radiation or the energy of the ejected photoelectron contains information about the nature of the core hole created, including information about the vibrational levels of the core-hole state. In emission techniques, photons or electrons emitted in the process of filling the core hole are analyzed for that same information, hence the core-ionized molecule is the initial state of these systems. The techniques used to study the vibrational structure accompanying core-hole creation or filling are all limited or complicated by the nature of the initial or final states of the experiment.

At very high experimental resolutions, vibrational bands are often observed on the core to bound transitions (usually core  $\rightarrow$  antibonding) in the preedge region of photoabsorption (PAS) and electron-energy-loss (EELS) spectra.<sup>6,7</sup> The intensities and spacing of the vibrational bands are influenced by both the core hole and the presence of the excited electron in an empty orbital of the valence shell of the molecule. The bonding properties of the molecule, and hence the vibrational manifold of the core excitation are affected by these excited electrons. Vibrational fine structure has been resolved in the  $\text{N}1s \rightarrow 1\pi_g^*$  transition in the preedge of the N  $1s$  absorption spectrum of  $\text{N}_2$  by both EELS (Refs. 7 and 8) and very recently by PAS.<sup>6,9,10</sup> Spectral features resulting from excitations of the C  $1s$  electron into an antibonding  $\pi^*$  orbital also exhibit vibrational structure for the simple carbon compounds,  $\text{CO}$ ,<sup>11,12</sup>  $\text{CH}_4$ ,<sup>12,13</sup>  $\text{C}_2\text{H}_2$ ,<sup>13,14</sup>  $\text{C}_2\text{H}_4$ ,<sup>6,10,13-16</sup> and  $\text{C}_6\text{H}_6$  (Refs. 14 and 15) and the spectra have been resolved by both techniques. When vibrational structure is observed for the nonbonding Rydberg levels<sup>17</sup> it is possible to estimate the effect of the core hole on the bonding properties of the molecule since the Rydberg orbitals do not interact with the molecule appreciably.

X-ray emission,<sup>18,19</sup> Auger,<sup>20-22</sup> and autoionization<sup>21,23</sup> spectra are often complicated by interference between the finite lifetime of the core-hole state and its vibrational structure.<sup>24-26</sup> Emission studies of vibrations in core levels have concentrated primarily on simple diatomics such as  $\text{N}_2$ ,<sup>18,20,23</sup>  $\text{CO}$ ,<sup>18,21,27</sup>  $\text{NO}$ ,<sup>18</sup>  $\text{O}_2$ ,<sup>18,22</sup> and simple hydrides such as  $\text{H}_2\text{O}$ ,<sup>28</sup>  $\text{NH}_3$ ,<sup>29</sup> and  $\text{H}_2\text{S}$ .<sup>30</sup> One particular experimental advantage of the emission techniques is that a highly monochromatic excitation source is not usually required and often laboratory sources can be used.

The difficulties involved in obtaining vibrationally resolved core-level photoelectron spectra are primarily experimental. A highly monochromatic light source with much greater intensity than needed for photoabsorption spectroscopy is required to resolve vibrational bands spaced  $< 0.3$  eV apart at energies of usually  $> 100-300$

eV. This requirement has prevented core-level photoelectron spectra from being obtained with resolved vibrational structure in all but the simplest of compounds,  $\text{CH}_4$  (Refs. 1, 2, and 31) and  $\text{SiH}_4$ .<sup>32,33</sup> Using monochromatized Al  $K\alpha$  sources, the bandwidth of the incident radiation has previously been limited to  $>0.3$  eV. With the use of a high-resolution monochromator and a synchrotron radiation source, core-level photoelectron spectra can be used to study changes in the intensities of the vibrational bands as a function of energy of the incident light. With the other techniques listed above, vibrational structure appears only at discrete levels of fixed energy and therefore they cannot be used for such studies. Theoretical calculations have indicated that the relative intensities of vibrational bands within a photoelectron line should be affected by shape resonances in both valence and core levels.<sup>34</sup> Vibrationally resolved studies of valence photoelectron bands have confirmed this prediction in numerous systems<sup>35,36</sup> but to date there have been no reports of analogous studies performed using core-level-photoelectron spectroscopy. The recent commissioning of new high-resolution monochromators<sup>6,10,37</sup> and the future availability of new high brightness synchrotrons should facilitate such measurements in core levels. Overall, photoelectron spectroscopy can provide information about the nature of the core-hole ion that is not available from other techniques due to the lack of interaction between the ejected electron and the core-hole ion. In addition, it should be possible to obtain vibrationally resolved cross sections.

Vibrational fine structure observed in core-level spectroscopies is the result of differences in the equilibrium nuclear geometries of the initial and final states of the process which creates or fills a core hole. In the photoelectron experiment, for instance, the initial state is the ground vibrational state of the ground electronic state of the molecule. Under the Born-Oppenheimer approximation, which presumes separability of the nuclear and electronic parts of the wave function describing the molecule, the photoionization process involves only an electronic transition. The nuclear geometry of the final state remains unchanged from that of the initial state (neutral molecule) in the photoionization process (sudden approximation). The *equilibrium* nuclear geometry of the final state, however, may be different from the nuclear geometry of the initial state due to electronic reorganization resulting from the incomplete screening of the positive nucleus by the core hole. In quantum-mechanical terms, changes in the equilibrium nuclear geometry upon ionization allow for nonzero overlap between the vibrational ground state of the initial electronic state,  $v''=0$ , and higher vibrational states of the final electronic state,  $v'=0,1,2,\dots,n$ . Franck-Condon (FC) factors, defined as the square of the overlap integral between vibrational states of the initial and final electronic states of the transition, can be used to calculate the relative intensities of the individual vibrational bands in the manifold observed. Franck-Condon factors can be calculated only if the potential energy surfaces of the initial and final electronic states are known.

The spacings of the vibrational levels in the ionic core-

hole state often change from those of the neutral ground state as determined by the change in the potential energy surface of the final state. When vibrational structure is resolved for the core-hole state, energies of the vibrational levels can be determined and used in the calculation of the potential energy surface of the core-hole state. Individual vibrational states are usually not resolved in core-level photoelectron spectroscopy but rather the photoelectron line is asymmetrically broadened by contributions from unresolved vibrational bands.<sup>1</sup> In this situation, vibrational energy levels can be obtained by several different means; by deconvolution of the peak shape, a process which does not always yield one unique result; from theoretical calculations, which are often difficult and time consuming; or by use of the equivalent-cores approximation which often yields accurate results. In the equivalent-cores model, physical properties of the core-hole ion state of a molecule are approximated by the properties of a molecule in which the core ionized atom,  $Z$ , is replaced by one with an additional proton,  $Z+1$ . Removal of a core electron from the molecule has approximately the same effect on the valence electrons, and hence most of the chemical properties of the molecule, as the addition of a proton to the nucleus of the ionized atom. This is the basis of the equivalent-cores approximation. The equivalent-cores model has been applied to estimate core-electron binding-energy shifts using Jolly's thermodynamic interpretation,<sup>38,39</sup> and to aid in the assignment of core-level preedge spectral features.<sup>9,14,17,40</sup> The model has also been applied to approximate the potential energy surfaces of final states of core ionizations to estimate core-level linewidths<sup>41,42</sup> or to calculate parameters describing the vibrational fine structure of the core-ionized states.<sup>9,22,43</sup> Previous experimental<sup>1,33</sup> and theoretical<sup>44-46</sup> studies have established the applicability of the equivalent-cores approximation in the determination of vibrational energy levels for core-ionized molecules.

In the majority of the previous reports of vibrational fine structure observed in core-level spectroscopy, the  $K$ -shell spectra of simple diatomic, triatomic, or hydride molecules of first-row elements, C, N, O, and F, were examined for vibrational structure. Broad lines observed in the photoelectron spectra of molecular and atomic C, N, and O adsorbates on a Ni(100) substrate have been attributed to vibrational broadening.<sup>43,47-49</sup> Vibrational structure was observed in the  $LVV$  Auger spectrum of  $\text{H}_2\text{S}$  in one of the few studies of vibrational effects in core-level spectra of non-first-row elements.<sup>30</sup> More recently we reported the first vibrationally resolved photoelectron spectra of the Si  $2p$  levels of  $\text{SiH}_4$  (Refs. 32 and 33) and  $\text{SiF}_4$ .<sup>33</sup>

In this report we present high-resolution Si  $2p$  photoelectron spectra of eleven silicon molecules:  $\text{SiH}_4$ ,  $\text{C}_2\text{H}_5\text{SiH}_3$ ,  $(\text{CH}_3)_2\text{SiH}_2$ ,  $(\text{CH}_3)_3\text{SiH}$ ,  $(\text{CH}_3)_4\text{Si}$ ,  $\text{SiF}_4$ ,  $\text{SiCl}_4$ ,  $(\text{CH}_3)_3\text{SiCl}$ ,  $(\text{CH}_3)_3\text{SiI}$ ,  $\text{Cl}_2\text{SiH}_2$ , and  $\text{CH}_3\text{SiF}_3$ . All of the spectra exhibit vibrational structure and extensive use of the equivalent-cores approximation is made to estimate the energies of the vibrational levels. High-resolution photoelectron spectra of  $\text{SiH}_4$  and  $\text{SiF}_4$  were reported by us previously<sup>33</sup> and the spectrum of  $\text{SiH}_4$  is reproduced

here to illustrate the effect of experimental resolution on the observed vibrational structure. Experimental resolution plays a crucial role in the observation of vibrational structure and we will show that photon resolutions of  $\leq 0.2$  eV are required to resolve even the simplest structure. Accurate adiabatic Si 2p<sub>3/2</sub> ionization potentials are also reported for all of the compounds.

## II. EXPERIMENT

Samples of the eleven compounds used in this study were obtained commercially and liquid samples were degassed with repeated freeze-pump-thaw cycles. The samples were then introduced directly into the gas cell of the spectrometer at pressures of between 0.5 and 1.0 torr. Constant sample pressures were maintained over the time required to accumulate data for each spectrum.

The photoelectron spectrometer used to measure the spectra reported in this study has been described in detail elsewhere.<sup>32</sup> Briefly, the spectrometer consists of a McPherson 36-cm mean radius electron energy analyzer which scans the energies of the electrons emitted by the interaction of the monochromatized synchrotron beam with the sample in the gas cell. The analyzer is mounted at a pseudomagic angle with respect to the polarization vector of the synchrotron light in order to minimize the dependence of the measured intensities on the asymmetry parameter  $\beta$ .<sup>50</sup> Slits of 1 mm at the entrance and exit foci of the analyzer result in electron resolutions,  $\Delta E/E$  of  $\frac{1}{720}$ . Assorted pumping and differential pumping was used on the spectrometer and beamline to isolate the high-pressure region of the gas cell from the high-vacuum regions of the optical components of the beamline.

With the exception of the very high-resolution spectra of SiH<sub>4</sub>, SiF<sub>4</sub>, and Si(CH<sub>3</sub>)<sub>4</sub>, all of the photoelectron spectra reported here were measured with photons from the CSRF Mark IV grasshopper monochromator.<sup>51</sup> A 900 groove/mm grating was used in the monochromator, yielding a minimum practical photon resolution of 0.12 Å with 20 μm slit widths (0.16 eV at 130 eV photon energy). Monochromator slit widths were varied to yield the desired photon resolutions. The very high-resolution photoelectron spectra of SiH<sub>4</sub>, SiF<sub>4</sub>, and Si(CH<sub>3</sub>)<sub>4</sub> were measured with photons from the undulator monochromatized with the 6-m toroidal grating monochromator on the Aladdin storage ring.<sup>32</sup>

Vibrational structure in the photoelectron spectra was deconvoluted using a nonlinear least-squares method<sup>52</sup> employing a linear combination of Gaussian and Lorentzian line shapes. A single peak shape (half height width and Gauss/Lorentz ratio) split by the Si 2p spin-orbit coupling and vibrational splitting was used to describe the line shape for all of the experimental spectra. Anharmonic factors were not included in the fitting procedure, since only a small number of vibrational states were observed in most of the Si 2p photoelectron spectra. In cases where more vibrational states were found they were not individually resolved and anharmonic factors could not be determined.

## III. RESULTS AND DISCUSSION

Experimental Si 2p photoelectron spectra of the eleven compounds used in this study are presented in the figures and/or summarized in Table I for several different experimental resolutions. The experimental resolutions given in Table I were calculated from the formal photon and electron energy resolutions using  $\Gamma_{\text{experimental}}^2 = \Gamma_{\text{photon}}^2 + \Gamma_{\text{electron}}^2$ , where  $\Gamma$  represents the resolution or bandwidth. The experimental resolution in these spectra was varied by changing only the photon resolution, since the resolution of the electron energy analyzer is determined by the fixed entrance and exit slits. Very high-resolution ( $\Delta E \leq 0.1$  eV) spectra reported here were recorded for SiH<sub>4</sub>, SiF<sub>4</sub>, and Si(CH<sub>3</sub>)<sub>4</sub> using the undulator beamline since photon resolutions of that calibre were not possible with a 900 groove/mm grating in the grasshopper monochromator.

The simulated spectra plotted as solid lines in the figures are representations of the parameters describing the spectra determined from the least-squares fit to the experimental data. The spectra are described by a position which is the adiabatic ionization energy of the  $v'=0$  vibrational level, a line shape which is defined by the full width at half maximum (*FWHM*) of the peak and the proportion of Gaussian component (Gauss fraction) of the line shape, the Si 2p spin-orbit splitting, and one or more manifolds of vibrationally split bands. The vibrational manifolds are further defined by the spacing between the vibrational bands and the relative intensities of the bands. Numerical values of the fitted parameters are summarized in Table I for all of the molecules at the resolutions indicated.

### A. SiH<sub>4</sub>

Photoelectron spectra of the Si 2p levels of SiH<sub>4</sub> measured at four different photon energy resolutions are presented in Fig. 1. The highest resolution spectrum in Fig. 1(d) was measured with a photon energy of 135 eV while the lower resolution spectra were measured at 130 eV. The effect of photon resolution on the spectrum is evident, with formal resolutions of  $\leq 0.2$  eV required to resolve the fine structure of the Si 2p photoelectron line. The fine structure observed is due to both the Si 2p spin-orbit splitting and Si—H stretching vibrations.

Each of the four SiH<sub>4</sub> Si 2p photoelectron spectra were deconvoluted using the methods described. A summary of the parameters from these fits is given in Table I. Spin-orbit parameters for the Si 2p spectra of SiH<sub>4</sub>, as well as those for the other molecules in this report, were not constrained in the deconvolution process. The spin-orbit splitting was found to be  $0.617 \pm 0.005$  eV in the spectra for all of the molecules. The intensity ratios of the Si 2p<sub>1/2</sub> to Si 2p<sub>3/2</sub> photoelectron lines were found to range from 0.45 to 0.50 for all of the samples with the exception of SiCl<sub>4</sub> where the intensity ratio was found to be 0.41. The ionization energy of SiH<sub>4</sub> given in Table I, 107.31 eV, is the most accurately measured adiabatic ionization energy of the Si 2p<sub>3/2</sub> level for this molecule since other measurements of Si 2p binding energies were per-

formed using unmonochromatized Al  $K\alpha$  sources. Other values have been previously reported for the Si  $2p$  ionization potential of  $\text{SiH}_4$ , 107.14 eV (Ref. 53) and 107.31 eV,<sup>54</sup> measured at much lower experimental resolution ( $\geq 1.0$  eV). These values, however, correspond to the vertical ionization potential of  $\text{SiH}_4$  since vibrational and spin-orbit splittings of the Si  $2p$  level were not resolved previously. There is no simple comparison between the previously reported vertical ionization potentials and the adiabatic ionization energy since the vertical ionization potential is determined by a weighted average of the individual spin-orbit and vibrational levels.

The linewidths obtained from the deconvolution of the experimental spectra and listed in the Table are not always consistent with the experimental resolutions which are also given. In the higher resolution spectra,  $\Delta E = 98$  and 170 meV, the linewidths are greater than the formal experimental resolution due to contributions to the linewidth from the natural lifetime limited width of the Si

$2p$  core hole. In our previous report of the photoelectron spectrum of  $\text{SiH}_4$ , the natural linewidth of the Si  $2p$  core hole was found to be  $\sim 45$  meV from a line-shape analysis of the  $\text{SiH}_4$  spectrum.<sup>33</sup> In the lower resolution spectrum ( $\Delta E = 820$  meV) the linewidth is less than the formal resolution. This results from inaccuracies in the calibration of the slit widths and the inherent minimum resolution of the grasshopper monochromator.

Vibrational splittings resulting from the Si—H symmetric stretching vibration, and the relative intensities of the vibrational bands were allowed to freely fit the experimental data for the two highest resolution  $\text{SiH}_4$  Si  $2p$  photoelectron spectra. The values obtained are very similar despite the spectra being measured at different photon energies, 130 and 135 eV. The Si  $2p$  cross section is featureless in this energy region<sup>55</sup> and the vibrational band intensities are therefore not expected to change with the photon energy. Parameters determined for the  $\Delta E = 170$  meV spectrum were used in the deconvolution

TABLE I. Summary of the parameters describing the Si  $2p$  photoelectron spectra. Values were determined by a nonlinear-least-squares fit of the parameters to the experimental spectra, as described in the text.

Molecule	Si $2p_{3/2}$ binding energy (eV)	Experimental resolution $\Delta E$ (meV)	Observed linewidth (meV)	Gauss fraction	Vibrational splitting (meV)	Relative intensities of vibrational bands (tot=100)
$\text{SiH}_4$	107.31(5)	98	117	0.43	293	66,3,29,1,4,6
		170	232	1.0	295	65,30,5
		250	278	0.92	295	65,30,5
		820	590	1.0	295	65,30,5
$\text{Si}(\text{CH}_3)_4$	106.04(5)	99	242	0.68	81	41,24,17,10,5,3
		160	304	1.0	81	41,25,17,10,5,3
		380	358	0.86	81	41,25,17,10,5,3
		760	614	1.0	81	41,25,17,10,5,3
$\text{C}_2\text{H}_5\text{SiH}_3$	106.66(5)	170	248	0.86	290	64,31,5
					94	95,5
$(\text{CH}_3)_2\text{SiH}_2$	106.51(5)	160	280	1.0	287	56,27,11,5
					89	65,35
$(\text{CH}_3)_3\text{SiH}$	106.21(5)	160	289	0.77	284	85,15
					85	46,25,15,13
$\text{SiF}_4$	111.46(5)	96	116	0.95	105	1,2,6,13,18,20,17,12,7,3,1
		180	205	0.85	105	1,2,6,13,18,20,17,12,7,3,1
		250	250	0.80	105	1,2,6,13,18,20,17,12,7,3,1
		820	425	1.0	105	1,2,6,13,18,20,17,12,7,3,1
$\text{SiCl}_4$	110.18(5)	180	255	0.90	65	28,24,19,13,8,5,3
$(\text{CH}_3)_3\text{SiCl}$	107.12(5)	210	323	1.0	81	41,25,17,10,5,2
$(\text{CH}_3)_3\text{SiI}$	107.34(5)	250	359	1.0	81	41,25,17,10,5,2
$\text{Cl}_2\text{SiH}_2$	108.87(5)	200	384	1.0	287	79,17,4
$\text{CH}_3\text{SiF}_3$	109.69(5)	150	200	1.0	107	1,2,6,13,19,20,18,11,7,2,1

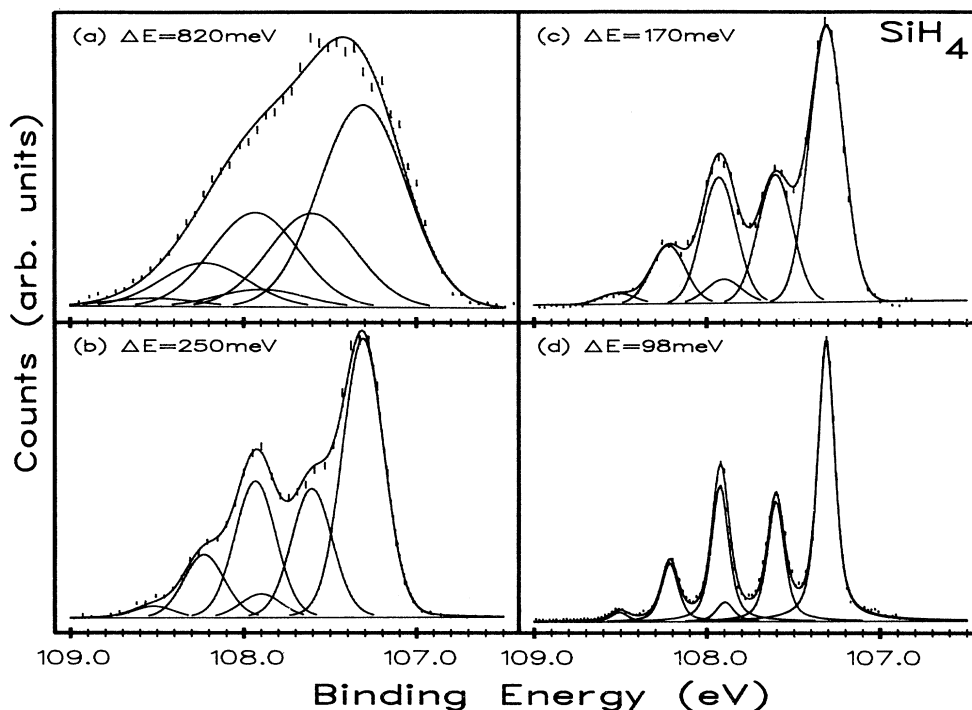


FIG. 1. Experimental photoelectron spectra of the Si 2p levels of silane, SiH<sub>4</sub> measured at formal experimental resolutions of (a) 820, (b) 250, (c) 170, and (d) 98 meV. The solid curves represent parameters which describe the peak shape convoluted with the Si 2p spin orbit and the Si—H vibrational splittings which were determined by fitting them to the experimental data using a least-squares method as described in the text. The parameters are summarized in Table I.

of the lower resolution spectra with only the linewidth and Gauss fraction allowed to change in the optimization procedure. The parameters obtained reproduce the spectra very well as indicated in Figs. 1(a) and 1(b).

The energy of the Si—H vibrations in Si 2p core-ionized SiH<sub>4</sub>, 2379 cm<sup>-1</sup> determined from the photoelectron spectrum, is larger than the vibrational energy of the ground electronic state, 2180 cm<sup>-1</sup> from infrared spectra,<sup>56</sup> indicating a change in the equilibrium nuclear geometry upon ionization of the ground-state molecule. The increased vibrational energy of the core-ionized state is consistent with a shortening of the Si—H bond in the ionic state. Ionization of core electrons has been found to result in a shortening of the bond in theoretical studies of core-level spectra of several other hydride molecules such as CH<sub>4</sub>,<sup>31</sup> NH<sub>3</sub>,<sup>29</sup> and H<sub>2</sub>S.<sup>30</sup> The vibrational energy of the core hole ion SiH<sub>4</sub><sup>+</sup> (Si 2p<sup>-1</sup>) supports the use of the equivalent-cores approximation to estimate vibrational energies in core-ionized molecules. The symmetric stretching frequency of PH<sub>4</sub><sup>+</sup>, 2295 cm<sup>-1</sup>,<sup>56</sup> closely approximates the value observed for the Si—H stretching frequency in SiH<sub>4</sub><sup>+</sup> (Si 2p<sup>-1</sup>). The symmetric stretching frequency of PH<sub>3</sub>, 2327 cm<sup>-1</sup>,<sup>56</sup> can also be used to approximate the Si—H stretching frequency of SiH<sub>4</sub> (Si 2p<sup>-1</sup>).

The effects of postcollision interaction (PCI) on the Si 2p photoelectron spectra presented in this study must be considered since the Si LVV Auger electrons have greater

kinetic energies than the Si 2p photoelectrons. The slower photoelectron can be considered to be overtaken by the faster Auger electron and subsequently shield it from the positive ion. This results in a gain of energy by the Auger electron and the loss of an equal amount of energy by the photoelectron.<sup>57</sup> Alternatively, the photoelectron can be thought to be “shaken-down” to a lower energy state.<sup>58</sup> Recapture of the photoelectron by the positive ion is even possible at low kinetic energies ( $\leq 2.0$  eV).<sup>59</sup> In a recent study of the  $N_5O_{23}O_{23}^1S_0$  Auger line of xenon measured using photon excitation with energies near the Xe 4d<sub>5/2</sub> threshold, the position of the line was found to shift by  $\sim 0.25$  eV from  $29.97 \pm 0.02$  eV at photon energies above 100 eV (where PCI does not affect the spectrum) to  $\sim 30.2$  eV when an excitation energy very near the Xe 4d<sub>5/2</sub> threshold was used.<sup>57,60</sup> The line shape of the  $N_5O_{23}O_{23}^1S_0$  Auger peak was observed to be asymmetrically broadened with a pronounced tail on the high kinetic-energy side of the peak when an excitation energy near the Xe 4d<sub>5/2</sub> threshold was used. The peak became narrower and more symmetric with increasing photon energy. While the effects of PCI on the shape and position of photoelectron peaks have not been measured directly, they should be equal in magnitude but of the opposite sign to those observed for the Auger-electron lines. The effect of PCI on the shapes and positions of the photoelectron peaks is complicated by the presence of more than one Auger decay contributing to the effect. Gen-

erally however, photoelectron lines are expected to be shifted to higher binding energy with noticeably asymmetric line shapes if PCI plays an important role in the high-resolution inner-shell spectra measured near the ionization threshold. The Si  $2p$  photoelectron lines of  $\text{SiH}_4$ , however, are very symmetric, implying that PCI does not significantly affect the spectra reported here. Further studies are definitely required to assess the importance of PCI in inner-shell photoelectron spectra of molecules, but in the spectra reported here the shape and position of the peaks are not noticeably distorted.

### B. $\text{Si}(\text{CH}_3)_4$

Photoelectron spectra of the Si  $2p$  levels of tetramethylsilane,  $\text{Si}(\text{CH}_3)_4$  are presented in Fig. 2 at a variety of experimental resolutions. The high-resolution  $\Delta E = 99$  meV spectrum [Fig. 2(d)] was measured at a photon energy of 135 eV while the other lower resolution spectra were measured at 129 eV. The  $\Delta E = 99$  meV spectrum is the highest resolution photoelectron spectrum of  $\text{Si}(\text{CH}_3)_4$  reported but even at this high resolution the Si  $2p$  lines appear as broad unresolved bands. The band shapes are asymmetric however, with a tailing of the band on the high-binding-energy side. Previously reported core-level photoelectron spectra of CO and  $\text{N}_2$  exhibited similar band shapes resulting from unresolved vibrational structure accompanying the core ionization.<sup>1</sup> Based on this and our previous observations of vibration-

al structure in the Si  $2p$  photoelectron spectra of  $\text{SiH}_4$  and  $\text{SiF}_4$  (Ref. 33) we propose that the Si  $2p$  photoelectron lines of  $\text{Si}(\text{CH}_3)_4$  are broadened by vibrational effects.

Without resolved vibrational structure, it is difficult to fit a vibrational series to the broad Si  $2p$  photoelectron lines. Using the equivalent-cores approximation, however, a reasonable estimate of the vibrational energy for the Si— $\text{CH}_3$  stretch of the core-ionized molecule can be obtained. The symmetric Si—C stretch is assumed to be the primary vibrational mode in the spectrum since the removal of a core electron can leave the molecule in an excited state of the symmetric stretch due to the change in bond distance caused by the ionization. According to the equivalent-cores model, symmetric P—C stretching energy of  $\text{P}(\text{CH}_3)_3$ ,  $653 \text{ cm}^{-1}$ , or  $\text{P}(\text{CH}_3)_4^+$ ,  $649 \text{ cm}^{-1}$  (0.081 eV) (Ref. 56) can be used to approximate the Si—C stretching frequency of Si  $2p$  core-ionized  $\text{Si}(\text{CH}_3)_4$  which has a symmetric stretching vibrational energy of  $593 \text{ cm}^{-1}$  in the ground electronic state.<sup>56</sup>

Parameters obtained from the deconvolution of the experimental Si  $2p$  photoelectron spectra of  $\text{Si}(\text{CH}_3)_4$  using the Si—C vibrational splitting determined above (0.081 eV) are summarized in Table I. The adiabatic ionization potential of the Si  $2p_{3/2}$  line was determined to be 106.04 eV using the vibrational manifold illustrated in Fig. 2. Previous values 105.94,<sup>61</sup> 105.82,<sup>53</sup> and 106.02<sup>62</sup> obtained using unmonochromatized Al  $K\alpha$  sources, are all in agreement with the value reported here.

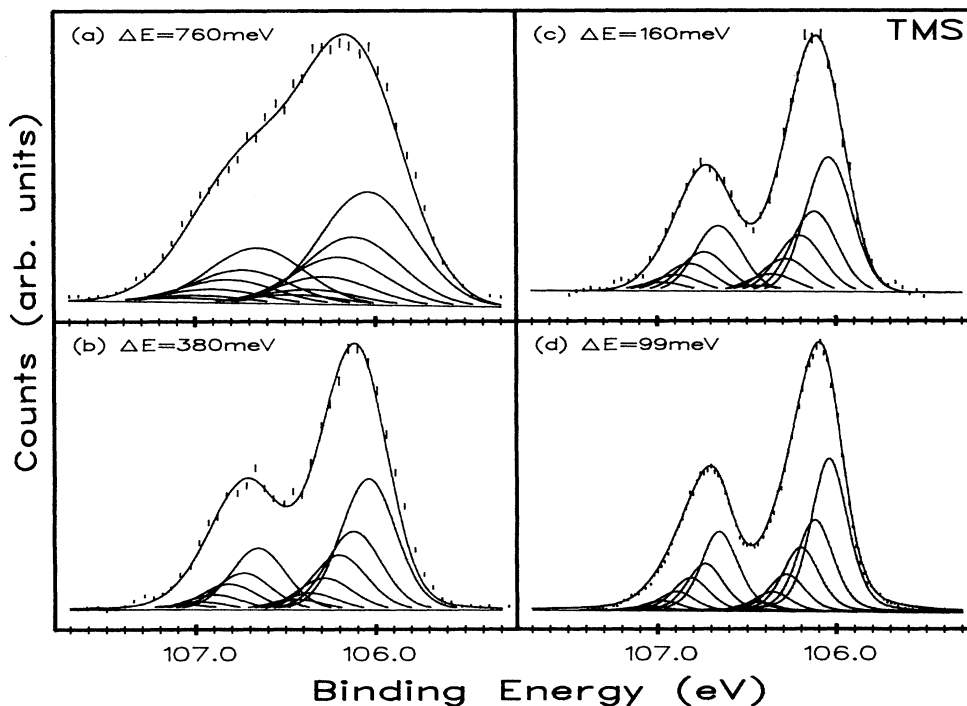


FIG. 2. Experimental photoelectron spectra of the Si  $2p$  levels of tetramethylsilane  $\text{Si}(\text{CH}_3)_4$  measured at formal experimental resolutions of (a) 760, (b) 380, (c) 160, and (d) 99 meV. The solid curves represent fitted parameters (Table I) as in Fig. 1.

Linewidths of the individual vibrational bands in the Si 2p photoelectron spectrum of Si(CH<sub>3</sub>)<sub>4</sub> were found to be 0.242 eV (Table I). These linewidths are much broader than those observed in the Si 2p photoelectron spectrum of SiH<sub>4</sub>, where 0.117 eV lines were found to reproduce the shape of the individually resolved vibrational bands. The broader linewidths for Si(CH<sub>3</sub>)<sub>4</sub> could be the result of either lifetime effects of the Si 2p core hole<sup>3,4,63</sup> or an incomplete description of the vibrational structure of the photoelectron spectra using only one vibrational mode. A relationship between the valence electron density surrounding the atom on which the core hole is created and the lifetime of the hole state has been proposed<sup>3,4</sup> and recently updated<sup>63</sup> to account for broadening of spectral lines corresponding to core excitations. Since the methyl ligands donate electron density to the silicon atom, illustrated by the lowering of the Si 2p binding energy of Si(CH<sub>3</sub>)<sub>4</sub> relative to SiH<sub>4</sub>, the lifetime of the Si 2p hole state will be shorter than that of the Si 2p hole state in SiH<sub>4</sub>. The corresponding photoelectron line should therefore be broader according to the assertion that an increased Auger decay rate of the core hole will result from the increased electron density on the silicon atom thereby shorting the lifetime of the core-hole state. Alternatively, the broad lines from the deconvolution of the data could be the result of an incomplete description of the vibrational states excited in the ionization process using the parameters chosen to fit the spectrum. Since the Si(CH<sub>3</sub>)<sub>4</sub> molecule is relatively complex with 17 atoms and 16 chemical bonds, numerous other vibrational modes such as C—H stretching, CH<sub>2</sub> wagging, etc., could also be responsible for some of the structure in the Si 2p photoelectron spectrum. In high-resolution photoabsorption spectra of C<sub>2</sub>H<sub>4</sub> and C<sub>6</sub>H<sub>6</sub> three different vibrational modes, C—H stretching, C—C stretching, and C—H bending, were identified with the aid of spectra of the deuterated compounds.<sup>6</sup> These spectra are complicated however, by the creation of a core hole leading to a lowering of the molecular symmetry since the carbon atoms are no longer equivalent in the core-excited species. If modes in addition to the Si—C stretch are also responsible for broadening the Si(CH<sub>3</sub>)<sub>4</sub> Si 2p photoionization spectrum, the deconvolution method will increase the widths of the vibrational bands to incorporate intensity from these modes.

The  $\Delta E = 160$  meV Si 2p photoelectron spectrum of Si(CH<sub>3</sub>)<sub>4</sub> was also deconvoluted using a vibrational splitting of 0.081 eV. Relative band intensities determined by the fitting procedure for this spectrum are almost identical to those determined for the  $\Delta E = 99$  meV spectrum (Table I). No excitation energy-dependent effects of the vibrational band intensities are observed nor expected since the Si 2p cross section for Si(CH<sub>3</sub>)<sub>4</sub> is relatively constant between 130 and 135 eV.<sup>64</sup> The other lower resolution spectra in Figs. 2(a) and 2(b) were fit using the vibrational manifold determined for the  $\Delta E = 160$  meV spectrum with only the linewidth and Gauss fraction allowed to change. Parameters resulting from the procedure with these constraints describe the spectra very well as evidenced by the close correspondence between the experimental and simulated spectra in Figs. 2(a) and 2(b).

### C. C<sub>2</sub>H<sub>5</sub>SiH<sub>3</sub>, (CH<sub>3</sub>)<sub>2</sub>SiH<sub>2</sub>, and (CH<sub>3</sub>)<sub>3</sub>SiH

Photoelectron spectra of the Si 2p levels of ethylsilane, C<sub>2</sub>H<sub>5</sub>SiH<sub>3</sub>, dimethylsilane, (CH<sub>3</sub>)<sub>2</sub>SiH<sub>2</sub>, and trimethylsilane, (CH<sub>3</sub>)<sub>3</sub>SiH, presented in Figs. 3(a)–3(c), were measured at photon energies of 130, 129, and 129 eV and total experimental resolutions of 170, 160, and 160 meV, respectively. The  $\Delta E = 160$  meV spectrum of Si(CH<sub>3</sub>)<sub>4</sub> has been included in Fig. 3(d) for comparison. Despite the less than optimum experimental resolution used in the measurement of these spectra [compared with the  $\Delta E = 0.1$  eV resolution attained for the spectra of SiH<sub>4</sub>, SiF<sub>4</sub>, and Si(CH<sub>3</sub>)<sub>4</sub>] they do exhibit interesting features which provide information about the nature of the Si 2p core-hole state in these molecules.

Inspection of the spectra in Fig. 3 shows that the Si 2p photoelectron spectra of C<sub>2</sub>H<sub>5</sub>SiH<sub>3</sub> [Fig. 3(a)] and SiH<sub>4</sub> [Fig. 1(c)—obtained at the same experimental resolution] are similar. Both spectra exhibit resolved vibrational structure, although it is slightly better resolved in the spectrum of SiH<sub>4</sub>. The Si 2p photoelectron spectrum of (CH<sub>3</sub>)<sub>2</sub>SiH<sub>2</sub> does not have resolved vibrational structure, but the highly asymmetric line shape extending over  $\sim 2.0$  eV indicates that vibrational structure must be responsible for the observed broadening. Finally, the spectrum of (CH<sub>3</sub>)<sub>3</sub>SiH in Fig. 3(c) appears to be very similar to the spectrum of Si(CH<sub>3</sub>)<sub>4</sub> in Fig. 3(d). The Si 2p spin-orbit split lines are more completely resolved in the Si 2p spectrum of Si(CH<sub>3</sub>)<sub>4</sub> than in the spectrum of (CH<sub>3</sub>)<sub>3</sub>SiH, indicating that more vibrational bands are present in the spectrum of the latter. Gradual changes in the shape of the Si 2p photoelectron spectra over the alkyl-silane molecular series suggest that two separate vibrational sequences cause the asymmetric line broadening in the mixed compounds. The experimental spectra of the mixed alkyl silanes were therefore deconvoluted using two vibrational sequences, one for bands corresponding to the Si—H stretch and another for bands resulting from the Si—C stretch.

Vibrational energies of suitable equivalent-cores molecules, C<sub>2</sub>H<sub>5</sub>PH<sub>3</sub><sup>+</sup>, etc., could not be found and so a different method was used to estimate the Si—H and Si—C vibrational frequencies in the core-ionized states of the molecules. In order to determine the appropriate vibrational splittings to use in the fitting procedure, vibrational frequencies of the ground-state neutral molecules were examined. The energy of the Si—H stretch changes from 2180 cm<sup>-1</sup> for SiH<sub>4</sub> to 2168 cm<sup>-1</sup> for CH<sub>3</sub>SiH<sub>3</sub>, to 2143 cm<sup>-1</sup> for (CH<sub>3</sub>)<sub>2</sub>SiH<sub>2</sub>, and finally to 2123 cm<sup>-1</sup> for (CH<sub>3</sub>)<sub>3</sub>SiH.<sup>56</sup> Rather than use these values directly to fit the vibrational structure in the photoelectron spectra, relative changes of the vibrational energies were calculated (i.e.,  $\nu_{\text{Si—H}}(\text{CH}_3\text{SiH}_3)/\nu_{\text{Si—H}}(\text{SiH}_4) = 2168 \text{ cm}^{-1}/2180 \text{ cm}^{-1} = 0.9945$ ) and applied to the value of the Si—H stretching energy determined for the SiH<sub>4</sub> Si 2p photoelectron spectrum to determine the vibrational energy for the next molecule in the series [i.e.,  $\nu_{\text{Si—H}}(\text{CH}_3\text{SiH}_3) = \nu_{\text{Si—H}}^*(\text{SiH}_4) \times 0.9945 = 0.293 \text{ eV}$ ]. Energies of the Si—C stretching modes were similarly determined for the core-hole ions using the energy of the Si—C stretch in Si 2p ionized Si(CH<sub>3</sub>)<sub>4</sub> (0.081 eV) and the

sequence of symmetric Si—C stretching energies for the methyl silanes.<sup>56</sup> The resulting vibrational energies were used to fit the vibrational structure in the Si 2*p* photoelectron spectra in Figs. 3(a)–3(c) and the values are summarized in Table I. When two vibrational sequences are used to fit the photoelectron spectrum, as for the three mixed alkyl silanes, the vibrational sequences combine to yield numerous vibrational bands.

Parameters from the least-squares deconvolution of the experimental data result in an accurate description of the Si 2*p* photoelectron spectra of the mixed alkyl silanes as seen by the similarity of the experimental and calculated spectra in Figs. 3(a)–3(c). The combination of Si—C and Si—H stretching modes therefore appears to describe the Si 2*p* photoelectron spectra of the mixed alkyl silanes. Even the Si 2*p* photoelectron spectrum of (CH<sub>3</sub>)<sub>2</sub>SiH<sub>2</sub>, which extends over 2 eV [Fig. 3(b)] is reasonably well reproduced by the fitting procedure. These results support the use of the methods described above to obtain the Si—H and Si—C vibrational energies used in the deconvolution of the experimental Si 2*p* photoelectron spectra. Parameters from the fitting procedure are summarized in Table I. The Si 2*p* binding energies listed compare reasonably well with previous results;<sup>54</sup> CH<sub>3</sub>SiH<sub>3</sub>, 106.95 eV; (CH<sub>3</sub>)<sub>2</sub>SiH<sub>2</sub>, 106.71 eV; (CH<sub>3</sub>)<sub>3</sub>SiH, 106.18 eV; and further illustrate the electron donating properties of the alkyl ligands.

The Si 2*p* linewidths obtained from the fitting procedure increase with the number of alkyl ligands on the

central silicon atom (Table I). The changing linewidths could be due to chemical effects on the lifetime of the core-hole state or an incomplete description of the vibrational structure of the Si 2*p* bands with only two vibrational modes. The increasing linewidths of the alkyl silanes with the number of alkyl ligands parallels the increased electron density on the central silicon atom. The variation in linewidth observed here, from 0.232 eV for SiH<sub>4</sub>, to 0.280 eV for (CH<sub>3</sub>)<sub>2</sub>SiH<sub>2</sub>, to 0.304 eV for Si(CH<sub>3</sub>)<sub>4</sub> (all from the  $\Delta E \approx 160$  meV spectra), is large when compared with the variation in the theoretical C 1*s* linewidths of a variety of carbon compounds.<sup>63</sup>

The increased linewidth observed for the alkyl silanes could also be the result of vibrational modes in addition to the Si—H and Si—C stretching modes contributing to the linewidths. The molecular structures of the alkylsilane molecules are considerably more complex than that of silane. Ionization of the silicon atom could create an attractive potential for the valence electrons of the alkyl groups bonded to it thereby withdrawing electron density from the carbon atoms. The equilibrium nuclear geometries of the methyl ligands might therefore be changed by the removal of the Si 2*p* electron and bands corresponding to vibrations within the alkyl groups could result. Vibrational bands at energies corresponding to the C—H stretch ( $\sim 0.4$  eV) might be expected in this case, but none are observed. The broadening of the photoelectron lines is probably due to a combination of the above two effects, decreased Si 2*p* core-hole lifetimes and

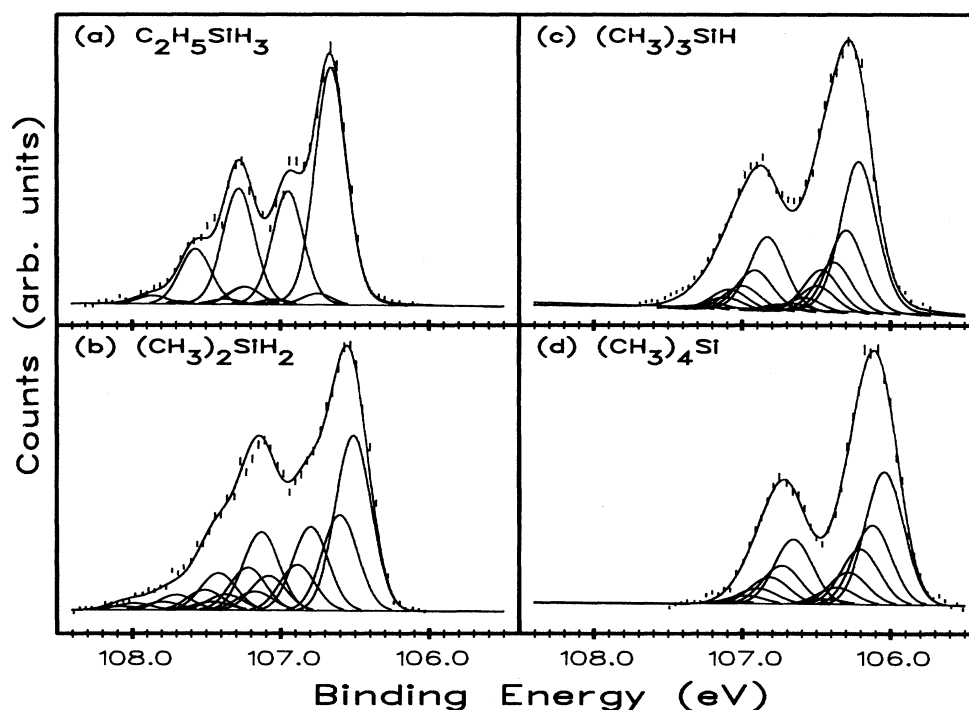


FIG. 3. Experimental photoelectron spectra of the Si 2*p* levels of (a) ethylsilane C<sub>2</sub>H<sub>5</sub>SiH<sub>3</sub>, (b) dimethylsilane (CH<sub>3</sub>)<sub>2</sub>SiH<sub>2</sub>, (c) trimethylsilane (CH<sub>3</sub>)<sub>3</sub>SiH, and (d) tetramethylsilane (CH<sub>3</sub>)<sub>4</sub>Si. All of the spectra were obtained with total experimental resolutions of  $\sim 0.2$  eV. Solid lines represent the fit of parameters (Table I) to the experimental spectrum as described in the text.

additional vibrational modes, but spectra measured at much better experimental resolutions must be obtained to determine their relative importance.

#### D. SiF<sub>4</sub>

Photoelectron spectra of the Si 2p levels of SiF<sub>4</sub> were measured using a variety of experimental resolutions and all of the spectra are very similar to our previously reported high-resolution spectrum.<sup>33</sup> Vibrational fine structure was resolved in only the high-resolution  $\Delta E = 96$  meV spectrum. The high-resolution spectrum was measured at 135 eV while the others were measured using a photon energy of 130 eV.

The experimental spectra were deconvoluted with a manifold of eleven vibrational bands spaced 0.105 eV apart, which is consistent with our previous report.<sup>33</sup> All eleven bands are necessary to properly deconvolute the high-resolution spectrum. The high-vibrational-level bands ( $v' = 9$  and 10) are required to account for intensity observed in the spectrum above a binding energy of  $\sim 113$  eV. Similarly, low-vibrational-level bands are required to reproduce the low intensity in the photoelectron band below  $\sim 111.6$  eV. The simulated spectrum, constructed by plotting the fitted parameters, reproduces the experimental data very well, supporting the assignment of eleven vibrational bands to the Si 2p photoelectron spectrum of SiF<sub>4</sub>. As the vibrational structure is not resolved in the other SiF<sub>4</sub> Si 2p photoelectron spectra, the vibrational manifold determined for the high-resolution spectrum was used in the deconvolutions with only the linewidths and Gauss fractions allowed to vary. The different excitation energies used for the high-resolution spectra is not expected to significantly affect the vibrational intensities since the Si 2p cross section of SiF<sub>4</sub> is relatively constant over this energy region.<sup>64</sup> Simply by increasing the linewidths of the vibrational bands and by changing the Gaussian component of the line shape, the lower resolution spectra are fit using the vibrational manifold determined for the higher resolution spectrum.

Linewidths obtained by the least-squares fits to the SiF<sub>4</sub> Si 2p photoelectron spectra are consistently narrower than those obtained for the spectra of SiH<sub>4</sub> measured at the same formal experimental resolutions. This is consistent with the changes predicted by the valence electron density theory used to estimate chemical effects on the natural linewidth,<sup>63</sup> since the highly electronegative fluorine ligands withdraw electron density from the central Si atom resulting in longer core-hole lifetimes.<sup>65</sup> Better experimental resolution is still required to individually resolve the vibrational bands in SiF<sub>4</sub> and unequivocally determine if there is truly a chemical effect resulting in different lifetime limited linewidths for Si 2p photoelectron spectra of SiH<sub>4</sub> and SiF<sub>4</sub>.

The  $\sim 5\%$  increase in the energy of the Si—F stretch in the core-ionized species ( $847\text{ cm}^{-1}$ ) relative to the ground state ( $800.8\text{ cm}^{-1}$ ) (Ref. 56) indicates that the removal of a Si 2p electron strengthens the Si—F bond. Our previous analysis of the vibrational energies in Si 2p ionized SiH<sub>4</sub> showed that the Si—H bond is also strengthened in the core-ionized species, where a  $\sim 10\%$

increase in the vibrational energy is observed.<sup>33</sup> The very broad distribution of vibrational bands observed in the Si 2p photoelectron spectrum of SiF<sub>4</sub>, extending over 1.1 eV, is consistent with very broad F 1s photoelectron linewidths observed previously.<sup>42,66</sup> It is also broader than the vibrational manifolds observed for SiH<sub>4</sub> and Si(CH<sub>3</sub>)<sub>4</sub> which are  $\sim 0.7$  eV wide. The Si 2p photoelectron spectrum of SiF<sub>4</sub> is also unique (within this group of eleven compounds) since the  $v' = 0$  band is not the most intense vibrational band within the vibrational manifold. This intensity distribution is consistent with a large change in the equilibrium geometry of the core-ionized state resulting in a poor overlap between the  $v' = 0$  and  $v'' = 0$  ground vibrational states of the final and initial electronic states, respectively. It is not possible to determine whether the change corresponds to a shortening or lengthening of the Si—F bonds without theoretical calculations. Previous calculations for first-row compounds have found that bond lengths decrease when a 1s electron is removed from a carbon or nitrogen atom, but increase when an oxygen or F 1s electron is involved.<sup>67</sup> The trend in bond length changes for second-row atoms is not known.

#### E. SiCl<sub>4</sub>

Three Si 2p photoelectron spectra of SiCl<sub>4</sub> are presented in Fig. 4. The spectra were measured at a photon energy of 130 eV. The overall resolution of the two Si 2p spin-orbit peaks does not change significantly with the formal experimental resolution over the three different resolutions used, with the region between the spin-orbit peaks always resolved to approximately half the height of the Si 2p<sub>1/2</sub> peak. Vibrational broadening causes the lack of sensitivity of the spectral resolution to the formal resolution and the same methods as those employed previously were used to fit a manifold of vibrational peaks to the spectra.

The applicability of the equivalent-cores approximation has been demonstrated in this study and it is used here to approximate the Si—Cl vibrational frequency of the Si 2p ionized molecule. The energy of the P—Cl symmetric stretch in PCl<sub>3</sub> is 0.065 eV, and this value was used in the deconvolution of the experimental SiCl<sub>4</sub> Si 2p photoelectron spectrum. The adiabatic ionization potential of the Si 2p<sub>3/2</sub> level of SiCl<sub>4</sub> was found to be 110.18 eV in the least-squares procedure, a value which compares favorably with previously reported values of 110.17 (Refs. 61 and 62) and 110.25 eV.<sup>53</sup> The fitted peak shape resulting from the least-squares fit of the vibrational manifold reproduces the experimental line shape, as illustrated in Fig. 4(d).

The Si 2p photoelectron spectra of SiCl<sub>4</sub> with formal experimental resolutions of 440, 220, and 180 meV were also deconvoluted using only two bands as illustrated in Figs. 4(a)–4(c). Two bands, representing the Si 2p<sub>3/2</sub> and 2p<sub>1/2</sub> photoelectron lines, were fit to the experimental spectra to determine the effects of the unresolved vibrational structure on the line shapes of the photoelectron lines. Parameters for the two bands (position, height, FWHM, and Gauss fraction) were not constrained in the

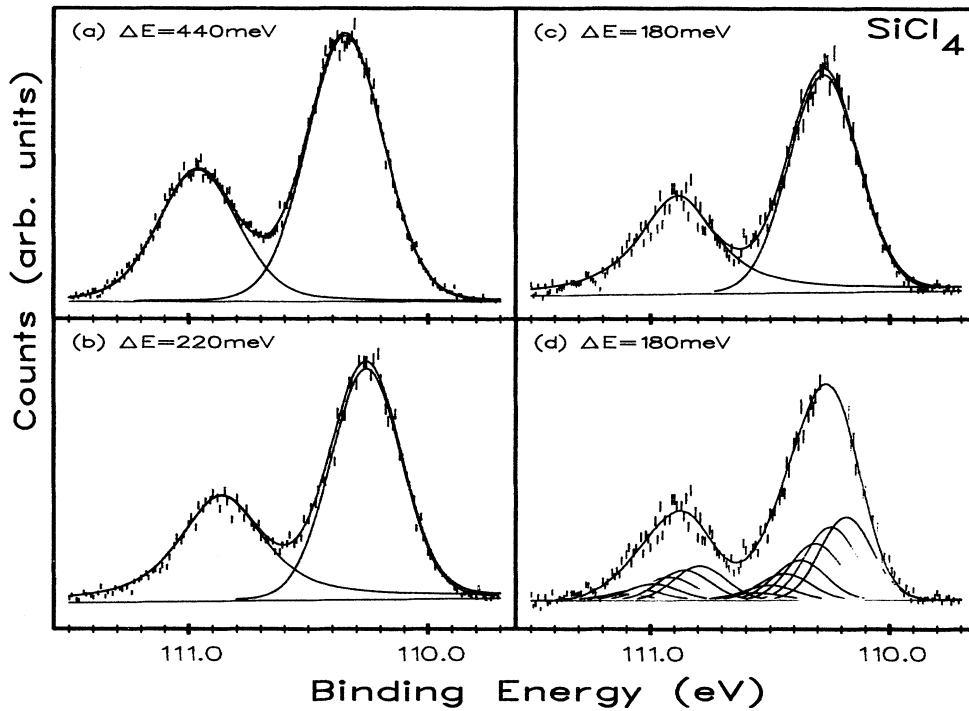


FIG. 4. Experimental photoelectron spectra of the Si  $2p$  levels of tetrachlorosilane  $\text{SiCl}_4$  measured at formal experimental resolutions of (a) 440, (b) 220, (c) 180, and (d) 180 meV. Solid curves in (a)–(c) represent the fit of two independently determined lines to the experimental data as described in the text. The solid curves in (d) represent the fitted parameters (Table I) as in Fig. 1.

least-squares procedure. The FWHM's and Gauss fractions obtained for the two bands are listed in Table II. Several trends are apparent from this data. For the Si  $2p_{3/2}$  photoelectron line, the linewidth decreases and the Gauss fraction increases as the experimental resolution is improved. The Si  $2p_{1/2}$  linewidth does not change significantly with experimental resolution, but the Gauss fraction decreases markedly as the resolution is improved. These differences are the result of the unresolved vibrational structure of the Si  $2p$  photoelectron lines.

These considerations are very important for distinguishing vibrational broadening where the spin-orbit doublet and vibrational splitting are not well resolved and further discussion is warranted to clarify these different widths and shapes. In the deconvolution of the photoelectron spectra, nonoverlapping regions of the spectrum dominate the fit of a band to the experimental spectrum. In the two-band deconvolutions of the  $\text{SiCl}_4$  Si  $2p$  photoelectron spectra, the high-binding-energy portion of the Si  $2p_{3/2}$  photoelectron line overlaps with the low-energy portion of the Si  $2p_{1/2}$  line. The least-squares procedure for the Si  $2p_{3/2}$  line is therefore dominated by the  $v'=0$  vibrational band at the low-binding-energy side of the band. The shape of the leading edge of the ground-state vibrational band is determined primarily by the lifetime of the Si  $2p$  core hole and resolution of the excitation source. In this experiment, where the photon width is greater than the lifetime width, the shape of the low-binding-energy side of the Si  $2p_{3/2}$  line is determined pri-

marily by the photon bandwidth. When the photon resolution used to measure the spectrum is improved therefore, so should the width of the Si  $2p_{3/2}$  photoelectron line decrease using a two-band fit. The Gauss fraction increases with improved photon resolution because contributions from higher vibrational bands ( $v'=1,2$ ) overlap with the ground vibrational band since the levels are so closely spaced. When the resolution is improved, the degree of overlap of the higher vibrational bands with the ground-state band decreases and the leading edge of the photoelectron line becomes sharper. The Si  $2p_{1/2}$  line is dominated by the high-energy portion of the band in the deconvolution procedure which encompasses the higher levels of the vibrational manifold. When a single line is used to deconvolute the Si  $2p_{1/2}$  photoelectron line therefore, the shape and breadth of the line will depend more

TABLE II. Summary of the peak widths (FWHM's) and Gauss fractions for the Si  $2p$  bands of the  $\text{SiCl}_4$  photoelectron spectra in Figs. 4(a)–4(c).

$\Delta E$ (meV)	Si $2p_{3/2}$		Si $2p_{1/2}$	
	FWHM (meV)	Gauss fraction	FWHM (meV)	Gauss fraction
440	373	0.9332	391	0.7757
220	346	0.9691	412	0.3278
180	340	1.0000	381	0.2243

upon the extent of the vibrational manifold. The width of the line in the deconvolution will therefore not change significantly with improved photon resolution. Improved photon resolution does decrease the degree of overlap between adjacent vibrational bands and the overall shape of the band will therefore change. A single band fit to the Si 2p<sub>1/2</sub> line will also encompass the higher vibrational bands of the Si 2p<sub>3/2</sub> line since the shape of the line for the Si 2p<sub>3/2</sub> band is dominated by the  $\nu'=0$  line. As a result, when the photon resolution is improved, and the Si 2p<sub>3/2</sub> line becomes narrower and more Gaussian, the Lorentzian component of the Si 2p<sub>1/2</sub> line must also increase to encompass all of the higher vibrational level of the 2p<sub>3/2</sub> line.

#### F. (CH<sub>3</sub>)<sub>3</sub>SiCl, (CH<sub>3</sub>)<sub>3</sub>SiI, Cl<sub>2</sub>SiH<sub>2</sub>, and CH<sub>3</sub>SiF<sub>3</sub>

Photoelectron spectra of the Si 2p levels of (CH<sub>3</sub>)<sub>3</sub>SiCl, (CH<sub>3</sub>)<sub>3</sub>SiI, Cl<sub>2</sub>SiH<sub>2</sub>, and CH<sub>3</sub>SiF<sub>3</sub> were measured at 130, 130, 129, and 125 eV, respectively. The spectra were deconvoluted with manifolds of vibrational bands and the resulting parameters are summarized in Table I. Spectra of the trimethyl silicon halide compounds were both fit using the vibrational manifold determined for Si(CH<sub>3</sub>)<sub>4</sub> since the energy of the Si—C stretch is greater than both the Si—Cl and Si—I stretching energies. The Si 2p photoelectron spectra of both trimethylhalides are very similar to the spectrum of Si(CH<sub>3</sub>)<sub>4</sub> and the experimental spectra of the trimethylhalides are well reproduced by the fitted parameters. The vibrational structure of the Si 2p photoelectron spectrum of Cl<sub>2</sub>SiH<sub>2</sub> was assumed to be dominated by Si—H vibrational bands, with an increased linewidth to account for the Si—Cl vibrational bands. The experimental spectrum is well described by the parameters determined by a least-squares analysis using the above approximations. Finally, the Si 2p photoelectron spectrum of CH<sub>3</sub>SiF<sub>3</sub> was deconvoluted using a vibrational manifold very similar to the one determined for SiF<sub>4</sub> since the spectra appear to be very similar.

Intensities of particular vibrational bands in the Si 2p photoelectron spectra of mixed compounds roughly follow the number of the particular ligand. In the trimethylhalide silanes for example, the Si 2p photoelectron spectra are very similar to the spectrum of Si(CH<sub>3</sub>)<sub>4</sub> since vibrational bands from the three methyl ligands dominate the manifold of vibrational bands. The Si 2p photoelectron spectrum of (CH<sub>3</sub>)<sub>3</sub>SiH also has a very similar shape [Fig. 3(c)] for similar reasons, although in this case the Si—H vibrations are spaced far enough apart to have a noticeable effect on the spectral profile. The Si 2p photoelectron spectrum of CH<sub>3</sub>SiF<sub>3</sub> also illustrates this point since the three fluorines dominate the one methyl ligand and the spectrum is therefore very similar to that of SiF<sub>4</sub>.

#### IV. CONCLUSIONS

High-resolution Si 2p photoelectron spectra of eleven silicon compounds; SiH<sub>4</sub>, C<sub>2</sub>H<sub>5</sub>SiH<sub>3</sub>, (CH<sub>3</sub>)<sub>2</sub>SiH<sub>2</sub>, (CH<sub>3</sub>)<sub>3</sub>SiH, (CH<sub>3</sub>)<sub>4</sub>Si, SiF<sub>4</sub>, SiCl<sub>4</sub>, (CH<sub>3</sub>)<sub>3</sub>SiCl, (CH<sub>3</sub>)<sub>3</sub>SiI, Cl<sub>2</sub>SiH<sub>2</sub>, and CH<sub>3</sub>SiF<sub>3</sub> measured using monochromatized synchrotron radiation were reported. The spectra all exhibit vibrational structure although individual vibrational bands were resolved in the spectra of only a few of the compounds. Parameters describing the shape and position of the photoelectron lines were fit to the vibrational structure using a nonlinear-least-squares method. Very accurate adiabatic Si 2p ionization potentials were determined by this method. The equivalent-cores approximation was used to estimate the vibrational energies of the Si 2p core-ionized molecules. The equivalent-cores model was found to yield reasonably accurate vibrational energy levels for those spectra where vibrational fine structure was resolved. The effect of unresolved vibrational structure on the overall shape of the photoelectron lines was also examined as a function of the experimental resolution. Photoelectron lines with unresolved vibrational structure were found to be asymmetric, with a sharp onset at low-binding energy and a broad tail on the high-binding-energy side of the band.

Evidence for chemical effects on the Si 2p core-hole lifetimes were seen in the photoelectron spectra of the alkyl-silane molecules and in the spectrum of SiF<sub>4</sub>. Linewidths of the individual vibrational bands of the Si 2p photoelectron lines were found to increase with the number of alkyl ligands on the central silicon atom and decrease for SiF<sub>4</sub>. Electron density on the silicon atom increases with the number of alkyl ligands due to the electron donating properties of the alkyl groups. In SiF<sub>4</sub>, the highly electronegative fluorine ligands withdraw electron density from the central silicon atom. A correlation between the electron density on the silicon atom and the core-hole lifetime is consistent with previous theories describing the effects of valence electron density on the Auger decay rates and hence on the core-hole lifetimes. An incomplete description of the vibrational structure of the Si 2p spectra of the alkyl silanes could also account for some of the line broadening.

#### ACKNOWLEDGMENTS

The authors wish to thank J. N. Cutler for providing the high-resolution photoelectron spectrum of Si(CH<sub>3</sub>)<sub>4</sub> and L. L. Coatsworth for his helpful discussions on the nonlinear-least-squares procedures. We are also indebted to the staff at the Synchrotron Radiation Center (Stoughton) for their technical support. We are grateful for the funding provided by the National Research Council (NRC) of Canada and the Natural Sciences and Engineering Research Council of Canada (NSERC).

<sup>1</sup>U. Gelius, S. Svensson, H. Siegbahn, E. Basilier, Å. Faxälv, and K. Siegbahn, Chem. Phys. Lett. **28**, 1 (1974).

<sup>2</sup>U. Gelius, L. Asplund, E. Basilier, S. Hedman, K. Helenelund, and K. Siegbahn, Nucl. Instrum. Methods B **229**, 85 (1984).

<sup>3</sup>R. W. Shaw, Jr. and T. D. Thomas, Phys. Rev. Lett. **29**, 689 (1972).

<sup>4</sup>R. M. Friedman, J. Hudis, and M. L. Perlman, Phys. Rev. Lett. **29**, 692 (1972).

- <sup>5</sup>J. H. D. Eland, *Photoelectron Spectroscopy* (Wiley, New York, 1974).
- <sup>6</sup>C. T. Chen and F. Sette, *Phys. Scr.* **T31**, 119 (1990).
- <sup>7</sup>A. P. Hitchcock, *Phys. Scr.* **T31**, 159 (1990).
- <sup>8</sup>G. R. Wright, C. E. Brion, and M. J. Van der Wiel, *J. Electron Spectrosc. Relat. Phenom.* **1**, 457 (1973).
- <sup>9</sup>C. T. Chen, Y. Ma, and F. Sette, *Phys. Rev. A* **40**, 6737 (1989).
- <sup>10</sup>P. A. Heimann, F. Senf, W. McKinney, M. Howells, R. D. van Zee, L. J. Medhurst, T. Lauritzen, J. Chin, J. Meneghettis, W. Gath, H. Hogrefe, and D. A. Shirley, *Phys. Scr.* **T31**, 127 (1990).
- <sup>11</sup>S.-Y. Lee and C.-H. Lai, *Chem. Phys. Lett.* **167**, 255 (1990).
- <sup>12</sup>M. Tronc, G. C. King, R. C. Bradford, and F. H. Read, *J. Phys. B* **9**, L555 (1976).
- <sup>13</sup>M. Tronc, G. C. King, and F. H. Read, *J. Phys. B* **12**, 137 (1979).
- <sup>14</sup>A. P. Hitchcock and C. E. Brion, *J. Electron Spectrosc. Relat. Phenom.* **10**, 317 (1977).
- <sup>15</sup>Y. Ma, F. Sette, G. Meigs, S. Modesti, and C. T. Chen, *Phys. Rev. Lett.* **63**, 2044 (1989).
- <sup>16</sup>H. Rabus, D. Arvanitis, M. Domke, A. Puschmann, L. Wenzel, G. Comelli, G. Kaindl, and K. Baberschke, *Phys. Scr.* **T31**, 131 (1990).
- <sup>17</sup>W. H. E. Schwarz, *Chem. Phys.* **11**, 217 (1975).
- <sup>18</sup>H. Ågren, L. Selander, J. Nordgren, C. Nordling, and K. Siegbahn, *Chem. Phys.* **37**, 161 (1979).
- <sup>19</sup>J. Nordgren and N. Wassdahl, *Phys. Scr.* **T31**, 103 (1990).
- <sup>20</sup>R. Murphy, I.-W. Lyo, and W. Eberhardt, *J. Chem. Phys.* **88**, 6078 (1988).
- <sup>21</sup>N. Correia, A. Flores-Riveros, H. Ågren, K. Helenlund, L. Asplund, and U. Gelius, *J. Chem. Phys.* **83**, 2035 (1985).
- <sup>22</sup>T. X. Carroll and T. D. Thomas, *J. Chem. Phys.* **92**, 7171 (1990).
- <sup>23</sup>E. D. Poliakoff, L. A. Kelly, L. M. Duffy, B. Space, P. Roy, S. H. Southworth, and M. G. White, *J. Chem. Phys.* **89**, 4048 (1988).
- <sup>24</sup>N. Correia, A. Flores-Riveros, H. Ågren, L. Pettersson, M. Bäckström, and J. Nordgren, *J. Chem. Phys.* **83**, 2053 (1985).
- <sup>25</sup>T. X. Carroll, S. E. Anderson, L. Ungier, and T. D. Thomas, *Phys. Rev. Lett.* **58**, 867 (1987).
- <sup>26</sup>F. Kaspar, W. Domcke, and L. S. Cederbaum, *Chem. Phys.* **44**, 33 (1979).
- <sup>27</sup>F. K. Gel'Mukhanov, L. N. Mazalov, and A. V. Kondratenko, *Chem. Phys. Lett.* **46**, 133 (1977).
- <sup>28</sup>A. Cesar, H. Ågren, and V. Carravetta, *Phys. Rev. A* **40**, 187 (1989).
- <sup>29</sup>H. Ågren, J. Müller, and J. Nordgren, *J. Chem. Phys.* **72**, 4078 (1980).
- <sup>30</sup>A. Cesar, H. Ågren, A. Naves de Brito, S. Svensson, L. Karlsson, M. P. Keane, B. Wannberg, P. G. Fournier, and J. Fournier, *J. Chem. Phys.* **93**, 918 (1990).
- <sup>31</sup>L. Asplund, U. Gelius, S. Hedman, K. Helenlund, K. Siegbahn, and P. E. M. Siegbahn, *J. Phys. B* **18**, 1569 (1985).
- <sup>32</sup>J. D. Bozek, J. N. Cutler, G. M. Bancroft, L. L. Coatsworth, K. H. Tan, D. S. Yang, and R. G. Cavell, *Chem. Phys. Lett.* **165**, 1 (1990).
- <sup>33</sup>J. D. Bozek, G. M. Bancroft, J. N. Cutler, and K. H. Tan, *Phys. Rev. Lett.* **65**, 2757 (1990).
- <sup>34</sup>J. L. Dehmer, D. Dill, and S. Wallace, *Phys. Rev. Lett.* **43**, 1005 (1979).
- <sup>35</sup>J. B. West, A. C. Parr, B. E. Cole, D. L. Ederer, R. Stockbauer, and J. L. Dehmer, *J. Phys. B* **13**, L105 (1980).
- <sup>36</sup>T. A. Ferrett, A. C. Parr, S. H. Southworth, J. E. Hardis, and J. L. Dehmer, *J. Chem. Phys.* **90**, 1551 (1989).
- <sup>37</sup>C. T. Chen and F. Sette, *Rev. Sci. Instrum.* **60**, 1616 (1989).
- <sup>38</sup>W. L. Jolly and D. N. Hendrickson, *J. Amer. Chem. Soc.* **92**, 1863 (1970).
- <sup>39</sup>D. A. Shirley, *Chem. Phys. Lett.* **15**, 325 (1972).
- <sup>40</sup>W. H. E. Schwarz and R. J. Buenker, *Chem. Phys.* **13**, 153 (1976).
- <sup>41</sup>W. L. Jolly and T. F. Schaaf, *Chem. Phys. Lett.* **33**, 254 (1975).
- <sup>42</sup>D. J. Bristow and G. M. Bancroft, *J. Amer. Chem. Soc.* **105**, 5634 (1983).
- <sup>43</sup>A. Nilsson and N. Mårtensson, *Phys. Rev. Lett.* **63**, 1483 (1989).
- <sup>44</sup>D. T. Clark and J. Muller, *Theoret. Chim. Acta (Berlin)* **41**, 193 (1976).
- <sup>45</sup>W. H. E. Schwarz, *Chem. Phys. Lett.* **40**, 1 (1976).
- <sup>46</sup>D. T. Clark, I. W. Scanlan, and J. Muller, *Theoret. Chim. Acta (Berlin)* **35**, 341 (1974).
- <sup>47</sup>N. Mårtensson and A. Nilsson, *Surf. Sci.* **211**, 303 (1989).
- <sup>48</sup>A. Nilsson and N. Mårtensson, *Solid State Commun.* **70**, 923 (1989).
- <sup>49</sup>N. Mårtensson and A. Nilsson, *J. Electron Spectrosc. Relat. Phenom.* **52**, 1 (1990).
- <sup>50</sup>J. A. R. Samson, *Phil. Trans. R. Soc. (London) Ser. A* **268**, 141 (1970).
- <sup>51</sup>K. H. Tan, G. M. Bancroft, L. L. Coatsworth, and B. W. Yates, *Can. J. Phys.* **60**, 131 (1982).
- <sup>52</sup>R. I. Jennrich and P. F. Sampson, *Technometrics* **10**, 63 (1968).
- <sup>53</sup>W. B. Perry and W. L. Jolly, *Inorg. Chem.* **13**, 1211 (1974).
- <sup>54</sup>J. E. Drake, C. Riddle, B. Glavinčevski, K. Gorzelska, and H. E. Henderson, *Inorg. Chem.* **17**, 2333 (1978).
- <sup>55</sup>G. Cooper, T. Ibuki, and C. E. Brion, *Chem. Phys.* **140**, 147 (1990).
- <sup>56</sup>K. Nakamoto, *Infrared and Raman Spectra of Inorganic and Coordination Compounds*, 4th ed. (Wiley, Toronto, 1986).
- <sup>57</sup>V. Schmidt, *J. Phys. (Paris) Colloq.* **48**, C9-401 (1987).
- <sup>58</sup>K. Helenlund, U. Gelius, P. Froelich, and O. Gosinski, *J. Phys. B* **19**, 379 (1986).
- <sup>59</sup>W. Eberhardt, S. Bernstorff, H. W. Jochims, S. B. Whitfield, and B. Crasemann, *Phys. Rev. A* **38**, 3808 (1988).
- <sup>60</sup>M. Borst and V. Schmidt, *Phys. Rev. A* **33**, 4456 (1986).
- <sup>61</sup>P. Kelfve, B. Blomster, H. Siegbahn, K. Siegbahn, E. Sanhueza, and O. Gosinski, *Phys. Scr.* **21**, 75 (1980).
- <sup>62</sup>J. E. Drake, C. Riddle, and L. Coatsworth, *Can. J. Chem.* **53**, 3602 (1975).
- <sup>63</sup>M. A. Coville and T. D. Thomas (unpublished).
- <sup>64</sup>J. D. Bozek, G. M. Bancroft, and K. H. Tan, *Chem. Phys.* **145**, 131 (1990).
- <sup>65</sup>M. O. Krause, *J. Phys. Chem. Ref. Data* **8**, 307 (1979).
- <sup>66</sup>R. W. Shaw, Jr. and T. D. Thomas, *Chem. Phys. Lett.* **22**, 127 (1973).
- <sup>67</sup>O. Gosinski, J. Müller, E. Poulain, and H. Siegbahn, *Chem. Phys. Lett.* **55**, 407 (1978).